http://www.kidney-international.org

see commentary on page 375

Microvesicles derived from endothelial progenitor cells protect the kidney from ischemia–reperfusion injury by microRNA-dependent reprogramming of resident renal cells

Vincenzo Cantaluppi[1], Stefano Gatti[2], Davide Medica[1], Federico Figliolini[1], Stefania Bruno[1], Maria C. Deregibus[1], Andrea Sordi[2], Luigi Biancone[1], Ciro Tetta[3,4] and Giovanni Camussi[1]

[1]*Dialysis and Kidney Transplantation Unit, Department of Internal Medicine, Center for Experimental Medical Research (CeRMS) and Nephrology, University of Torino, Torino, Italy;* [2]*Center for Surgical Research, Fondazione IRCCS Cà Granda Ospedale Maggiore Policlinico, Milano, Italy;* [3]*Sis-Ter SpA, Palazzo Pignano (CR), Italy and* [4]*Fresenius Medical Care, Bad Homburg, Germany*

Endothelial progenitor cells are known to reverse acute kidney injury by paracrine mechanisms. We previously found that microvesicles released from these progenitor cells activate an angiogenic program in endothelial cells by horizontal mRNA transfer. Here, we tested whether these microvesicles prevent acute kidney injury in a rat model of ischemia–reperfusion injury. The RNA content of microvesicles was enriched in microRNAs (miRNAs) that modulate proliferation, angiogenesis, and apoptosis. After intravenous injection following ischemia–reperfusion, the microvesicles were localized within peritubular capillaries and tubular cells. This conferred functional and morphologic protection from acute kidney injury by enhanced tubular cell proliferation, reduced apoptosis, and leukocyte infiltration. Microvesicles also protected against progression of chronic kidney damage by inhibiting capillary rarefaction, glomerulosclerosis, and tubulointerstitial fibrosis. The renoprotective effect of microvesicles was lost after treatment with RNase, nonspecific miRNA depletion of microvesicles by Dicer knock-down in the progenitor cells, or depletion of pro-angiogenic miR-126 and miR-296 by transfection with specific miR-antagomirs. Thus, microvesicles derived from endothelial progenitor cells protect the kidney from ischemic acute injury by delivering their RNA content, the miRNA cargo of which contributes to reprogramming hypoxic resident renal cells to a regenerative program.

Kidney International (2012) **82,** 412–427; doi:10.1038/ki.2012.105; published online 11 April 2012

KEYWORDS: acute kidney injury; exosome; ischemia-reperfusion

Correspondence: *Giovanni Camussi, Cattedra di Nefrologia, Dipartimento di Medicina Interna, Ospedale Maggiore S. Giovanni Battista 'Molinette', Corso Dogliotti 14, 10126, Torino, Italy. E-mail: giovanni.camussi@unito.it*

Received 26 April 2011; revised 19 January 2012; accepted 24 January 2012; published online 11 April 2012

Ischemia–reperfusion is one of the main causes of acute kidney injury (AKI).[1,2] Therapeutic strategies aimed to inhibit ischemia–reperfusion injury (IRI) may potentially limit AKI and the development of chronic kidney disease (CKD).[3] Several studies addressed the role of bone marrow–derived and tissue-resident stem cells in the regeneration of ischemic kidneys.[4–7] Endothelial progenitors (EPCs) are circulating bone marrow–derived precursors able to localize within sites of tissue damage inducing regeneration.[8,9] EPCs are known to exert protective effects in experimental models of hindlimb ischemia, myocardial infarction, and glomerular diseases.[10–12] Moreover, it has been recently demonstrated that EPCs are recruited in the kidney after IRI and that they induce tissue repair via secretion of pro-angiogenic factors.[13–15] EPC paucity and dysfunction have been proposed as mechanisms of accelerated vascular injury in CKD patients.[16]

The regenerative effects of EPCs on ischemic tissues have been ascribed to paracrine mechanisms including the release of growth factors and microvesicles (MVs).[17,18] MVs are small particles derived from the endosomal compartment known to have an important role in cell-to-cell communication through the transfer of proteins, bioactive lipids, and RNA to target cells.[19–22] We recently demonstrated that MVs released from EPCs are internalized into endothelial cells activating an angiogenic program by horizontal transfer of mRNAs.[18]

The aim of this study was to evaluate whether MVs released from EPCs exert a protective effect in an experimental model of acute renal IRI. Moreover, we studied *in vitro* the mechanisms of MV protection from hypoxia-induced endothelial and epithelial kidney cell injury.

RESULTS

Characterization of EPC- and fibroblast-derived MVs

Transmission electron microscopy on EPCs revealed the shedding of MVs (Figure 1a and b) by a membrane-sorting process (Figure 1c). Purified MVs showed a homogenous

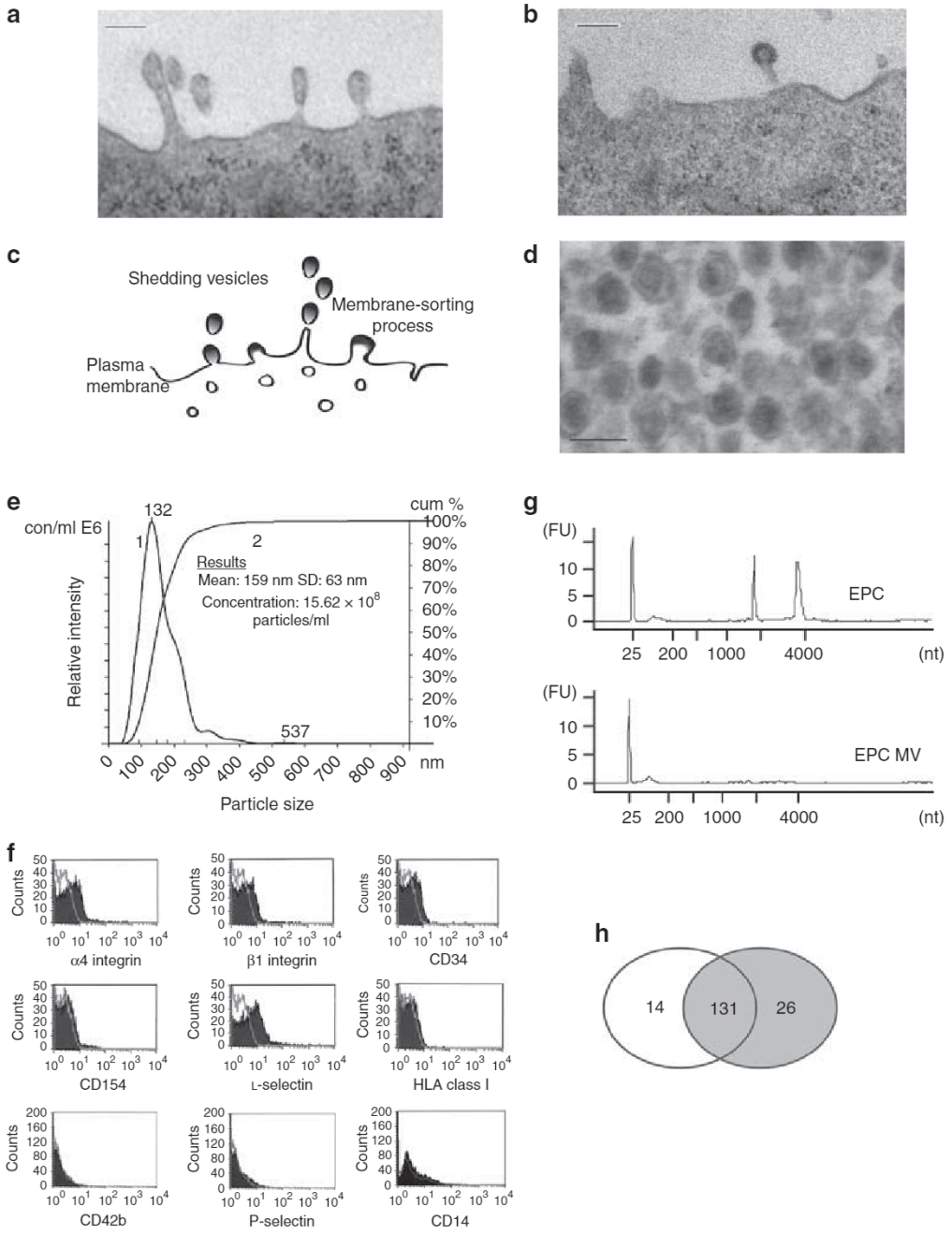

Figure 1 | Characterization of endothelial progenitor (EPC)-derived microvesicles (MVs). (**a**, **b**) Transmission electron microscopy performed on cultured EPCs showing MV shedding by a membrane-sorting process. (**c**) Schematic representation of shedding MV formation by budding of plasma membrane. (**d**) Transmission electron microscopy analysis of purified MVs showing a spheroid shape. In **a**, **b**, and **d**, bars indicate 100 nm. (**e**) Nanosight analysis of purified MVs: curve 1 describes the relationship between particle number distribution (left *Y* axis) and particle size (*X* axis); curve 2 describes the correlation between cumulative percentage distribution of particles (percentile in right *Y* axis) and particle size (*X* axis). Mean size and particle concentration values were calculated by the Nanoparticle Tracking Analysis (NTA) software that allows analysis of video images of the particle movement under Brownian motion captured by Nanosight LM10 and calculation of the diffusion coefficient, sphere equivalent, and hydrodynamic radius of particles by using the Strokes–Einstein equation. (**f**) Fluorescence-activated cell sorting (FACS) analysis of MV protein surface expression. (**g**) Bioanalyzer RNA profile of EPCs and EPC-derived MVs. (**h**) Analysis of microRNAs (miRNA array) present in EPCs and EPC-derived MVs (white circle: EPCs; gray circle: EPC-derived MVs).

pattern of spheroid particles. About 90% of MVs showed a size ranging from 60 to 160 nm (Figure 1d), whereas a minority of them were larger with a size around 1 μm. The purity and the size of EPC–MV preparations were confirmed by Nanosight analysis (Figure 1e). By fluorescence-activated cell sorting (FACS) analysis, EPC-derived MVs expressed α4

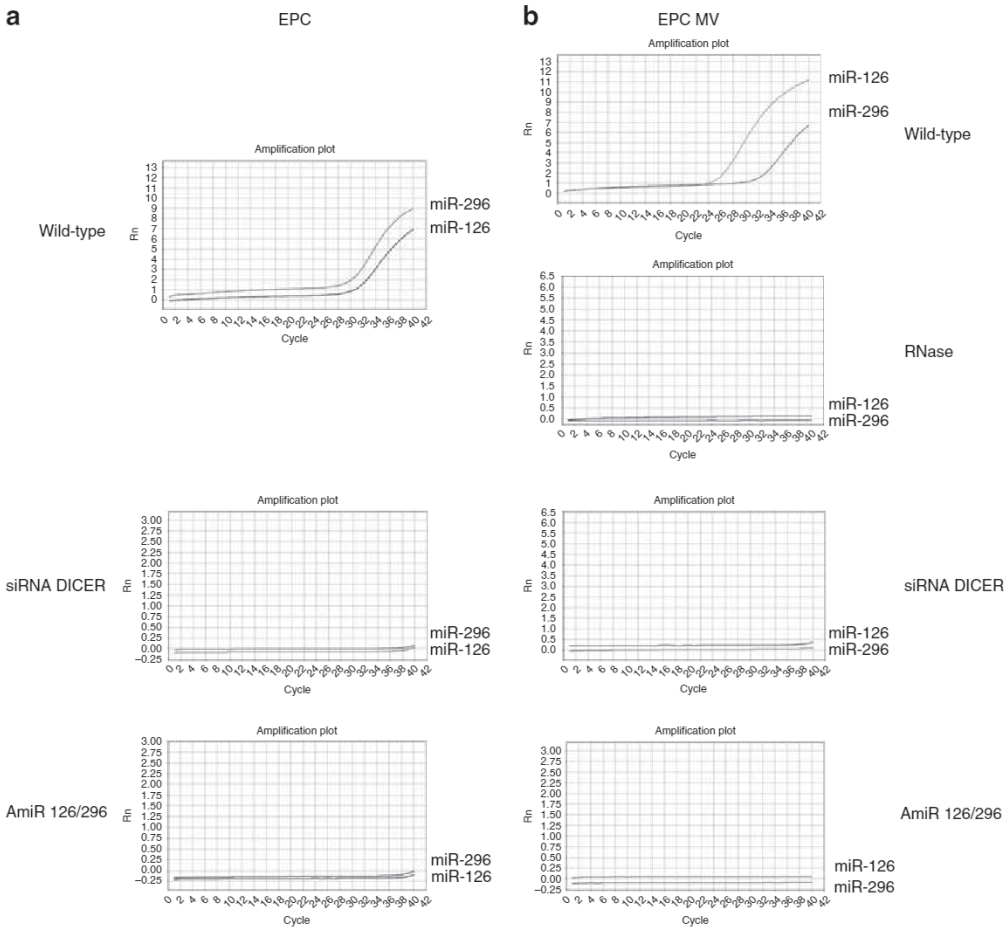

Figure 2 | Representative quantitative reverse transcriptase (qRT)-PCR for miR-126 and miR-296 in endothelial progenitors (EPCs) and EPC-derived microvesicles (MVs). (**a**) qRT-PCR analysis of miR-126 and miR-296 content in EPCs cultured with vehicle alone (wild-type), subjected to small interfering RNA (siRNA) for Dicer (siRNA Dicer), or transfected with anti-miR-126 and anti-miR-296 antagomiRs (AmiR 126/296). (**b**) qRT-PCR analysis of miR-126 and miR-296 content in MVs derived from EPCs cultured with vehicle alone (wild-type), treated with 1 U/ml RNase (RNase), subjected to siRNA for Dicer (siRNA Dicer), or transfected with anti-miR-126 and anti-miR-296 antagomiRs (AmiR 126/296).

and β1 integrin, CD154 (CD40-L), L-selectin and CD34 but not human leukocyte antigen class I and class II antigens and markers of platelets (P-selectin, CD42b) and monocytes (CD14) (Figure 1f). Bioanalyzer profile of EPC-derived MVs showed the presence of different subsets of RNAs and in particular enrichment for small RNAs, including microRNAs (miRNAs) (Figure 1g): miRNA array analysis showed the presence of 131 miRNAs shared by EPCs and EPC-derived MVs and 26 miRNAs specifically concentrated in MVs (Figure 1h, Supplementary Information Tables S1 and S2). The presence in EPCs and EPC-derived MVs of several pro-angiogenic and anti-apoptotic miRNAs, including miR-126 and miR-296, was confirmed by quantitative reverse transcriptase (qRT)-PCR with specific primer pairs (Figure 2). The expression of miR-126 and miR-296 seen by qRT-PCR was abrogated by RNase treatment of MVs and was absent in MVs derived from Dicer-silenced or antagomiR-transfected EPCs (Figure 2). MVs derived from fibroblasts were also characterized and used as negative experimental control. Fibroblast-derived MVs were larger than those of EPCs with a mean size of 260 nm detected by Nanosight (not shown). By FACS analysis, fibroblast-derived MVs expressed α4 and β1 integrin, CD154 and L-selectin, but not CD34, class I and class II human leukocyte antigens, and markers of platelets (P-selectin, CD42b) and monocytes (CD14) (Figure 3a and b). In comparison with EPC-derived MVs, fibroblast-derived MVs expressed significantly lower levels of L-selectin (Figure 3b). Bioanalyzer profile of fibroblast-derived MVs showed the presence of different subsets of RNAs including miRNAs (Figure 3c). The qRT-PCR analysis with specific primer pairs evidenced the absence of the pro-angiogenic miR-126 and miR-296 within fibroblast-derived MVs (Figure 3d).

Protective effect of EPC-derived MVs in experimental renal IRI

We evaluated the effects of EPC-derived MVs in an experimental model of acute renal IRI in Wistar rats (experimental

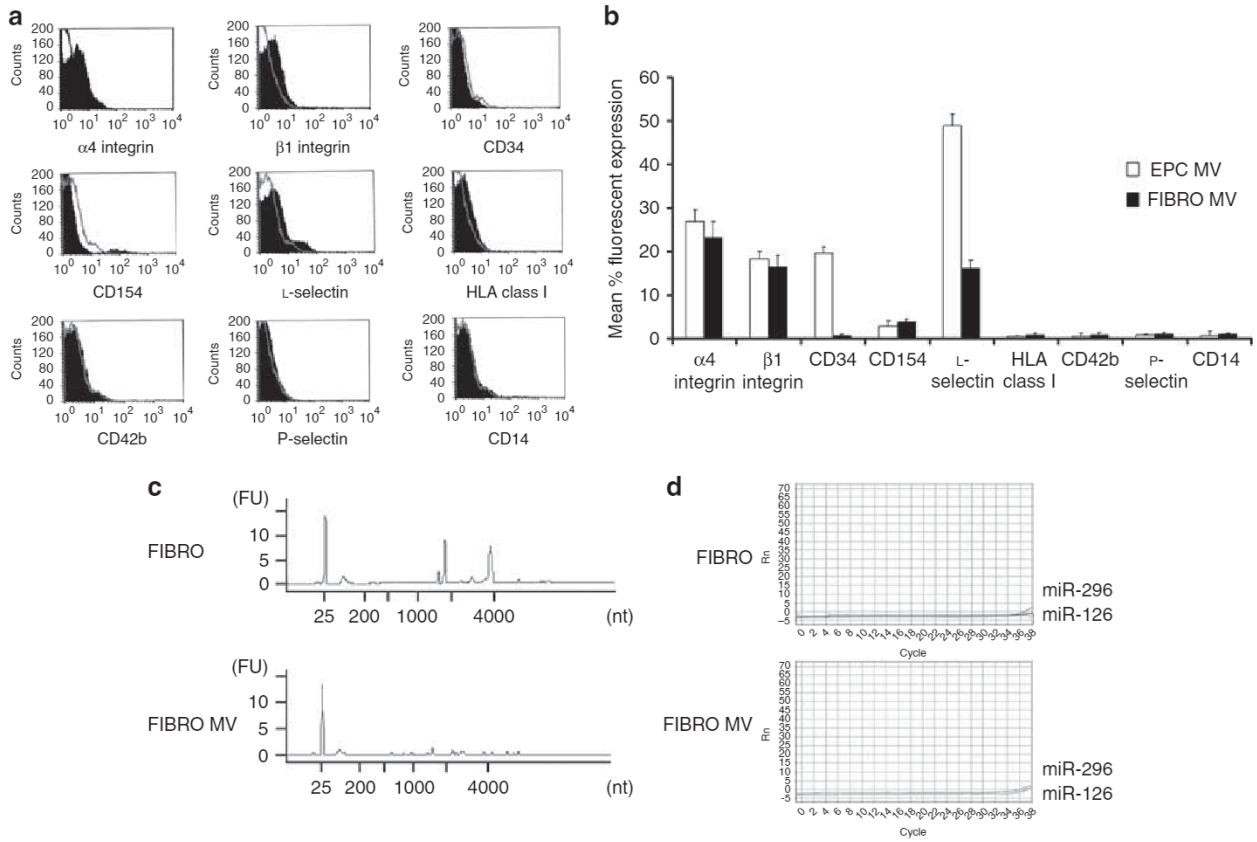

Figure 3 | Characterization of fibroblast-derived microvesicles (MVs). (**a**) Fluorescence-activated cell sorting (FACS) analysis of fibroblast-derived MV protein surface expression. (**b**) Comparison between FACS analysis of fibroblast- and endothelial progenitor (EPC)-derived MV protein surface expression. (**c**) Bioanalyzer RNA profiling of fibroblasts and fibroblast-derived MVs. (**d**) Representative quantitative reverse transcriptase (qRT)-PCR analysis for miR-126 and miR-296 in fibroblasts and fibroblast-derived MVs.

plan in Figure 4). In comparison with sham-operated animals, rats subjected to kidney IRI showed a significant rise in serum creatinine (Figure 5a) and blood urea nitrogen (BUN) (Figure 5b) that peaked at day 2 in association with histological signs of tubular injury such as formation of hyaline casts, vacuolization, widespread necrosis, and denudation of basal membrane (Figure 5c and Table 1). When rats were treated with EPC-derived MVs, a significant reduction of tubular lesions in parallel with the decrease in serum creatinine and BUN was observed at day 2 (Figure 5a–c and Table 1). The specificity of EPC-derived MVs was indicated by the absence of protective effect exerted by MVs derived from human fibroblasts (Figure 5a and b and Table 1). EPC-derived MVs enhanced the proliferation rate of tubular cells after IRI as detected by bromo deoxy uridine (Figure 6a and c) and proliferating cell nuclear antigen (Figure 6b and d) staining. Moreover, as shown by TdT-mediated dUTP nick end labeling assay (Figure 7a and b), MVs significantly reduced the number of apoptotic tubular cells. These renoprotective effects were significantly reduced when MVs were pre-treated with 1 U/ml RNase (Figures 5a–c, 6a–d, 7a–c and Table 1). When MVs derived from Dicer knocked-down EPCs or MVs released from EPCs transfected with anti-miR126 and anti-miR-296 antagomiRs were used, a significant reduction of the functional and histological protective effects on ischemic kidneys was also observed (Figures 5a–c, 6a–b, 7a and Table 1). Moreover, in comparison with sham-operated animals, IRI induced a massive infiltration of granulocytes (Figure 7c) and monocytes (Figure 7d) within kidneys. A significant decrease in leukocyte infiltration was observed in rats subjected to IRI and injected with MVs but not with RNase-treated MVs (Figure 7c and d). Similar functional and histological renoprotective effects of MVs were observed also at day 7 after IRI (not shown).

Six months after IRI, animals treated with MVs showed reduced levels of serum creatinine (Figure 8a), tubulointerstitial fibrosis, and glomerulosclerosis (Figure 8b), as well as a preserved expression of rat endothelial cell antigen-1 antigen in the tubulo-interstitial structures (Figure 8c and d) and within the glomeruli (Figure 8e and f), suggesting an inhibition of microvascular rarefaction and of progression toward CKD.

In biodistribution experiments, the accumulation of PKH26-labeled MVs was observed in the kidney 2 and 6 h after IRI. After 2 h, MVs were detectable within the endothelial cells of large vessels and within some peritubular capillaries and lumen of injured tubules (Figure 9a and b). After 6 h, the amount of tubular cells containing MVs was

markedly enhanced (Figure 9c). When injected in sham-operated control rats, the renal accumulation was significantly lower than in IRI, and only a slight staining for MVs was detected within glomeruli and tubular cells (Figure 9d). MVs were also detected in the liver of sham-operated controls, as well as in rats subjected to kidney IRI (Figure 9e).

In vitro effects of EPC-derived MVs on hypoxic peritubular endothelial cells (TEnCs) and tubular epithelial cells (TEpCs)

In consideration of the *in vivo* localization of MVs in peritubular capillaries and tubular cells, we evaluated the role of adhesion molecules in the internalization of MVs in isolated human TEnCs and TEpCs. MVs were efficiently internalized in TEnCs (Figure 9f) and TEpCs (Figure 9g). Moreover, hypoxia significantly enhanced MV internalization in both cell types (Figure 9h and i). Experiments conducted with blocking antibodies revealed that L-selectin was the main mediator of MV internalization in hypoxic cells (Figure 9h and i). Internalization was not altered in RNase-treated MVs (not shown). Control fibroblast-derived MVs showed a reduced internalization in normoxic and hypoxic TEnCs and TEpCs (Figure 10).

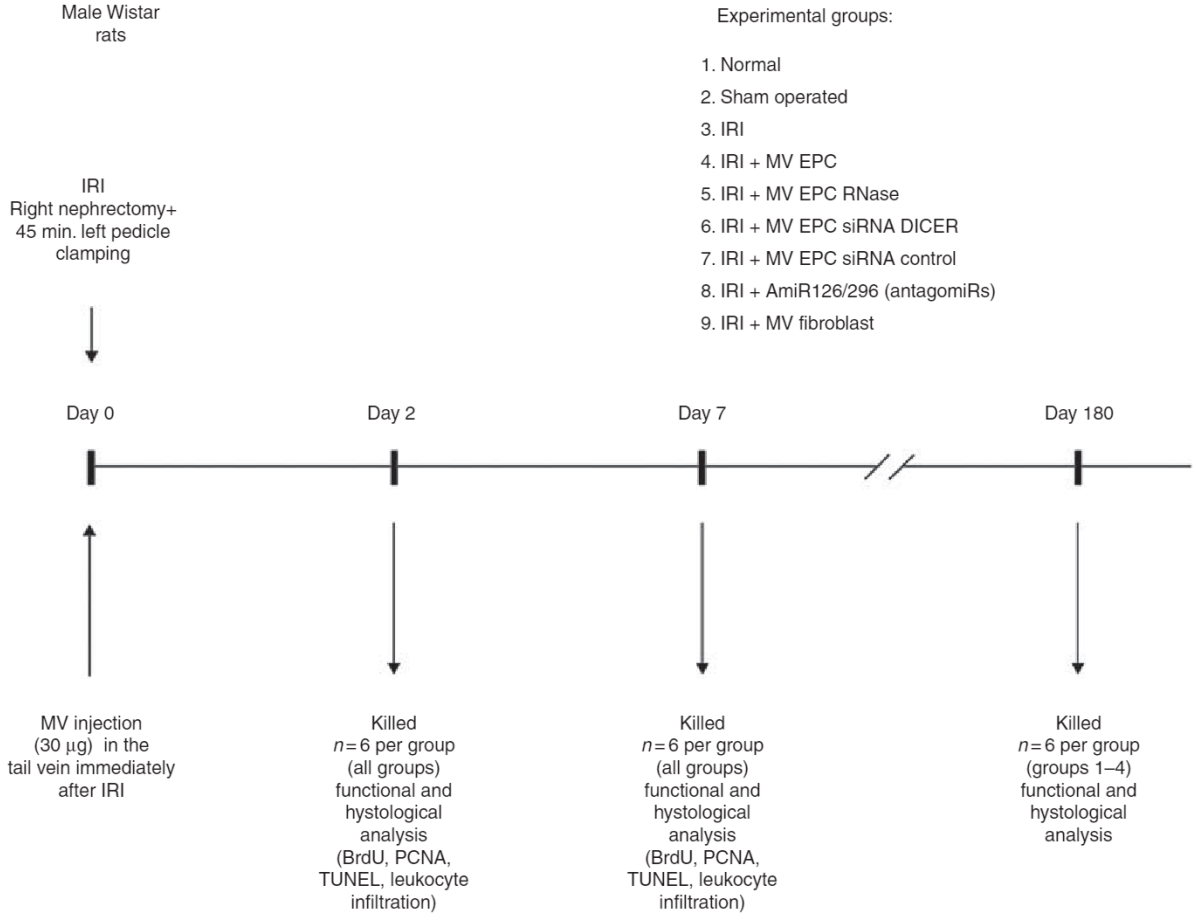

Figure 4 | Representative scheme of the experimental plan of acute renal ischemia–reperfusion injury (IRI) in male Wistar rats. Schematic representation of IRI model, experimental groups, number of animals treated, modality and dose of MV injection, timing of killing, and functional/histological analysis performed. BrdU, bromo deoxy uridine; EPC, endothelial progenitor; MV, microvesicle; PCNA, proliferating cell nuclear antigen.

Figure 5 | Protective effect of endothelial progenitor (EPC)-derived microvesicles (MVs) on acute kidney ischemia–reperfusion injury (IRI). (**a**, **b**) Evaluation of serum creatinine (**a**) and blood urea nitrogen (BUN) (**b**) in different experimental groups. IRI induced a significant increase in serum creatinine and BUN (*$P<0.05$ IRI vs. sham or normal). EPC-derived MVs significantly decreased serum creatinine and BUN ($^{\#}P<0.05$ IRI + MV EPC vs. IRI). The pre-treatment of EPC MVs with 1 U/ml RNase or the use of MVs released from EPCs transfected with small interfering RNA (siRNA) Dicer or with antagomiRs-126/296 (AmiR126/296) did not reduce serum creatinine and BUN ($^{\dagger}P<0.05$ IRI + MV EPC RNase, IRI + MV EPC siRNA DICER or IRI + MV EPC AmiR126/296 vs. IRI + MV EPC). MVs released from EPCs transfected with an irrelevant control siRNA (siRNA control) significantly decreased serum creatinine and BUN ($^{\#}P<0.05$ IRI + MV EPC siRNA control vs. IRI). The specificity of EPC-derived MVs was confirmed by the lack of renoprotective effect of MVs derived from control human fibroblasts ($^{\dagger}P<0.05$ IRI + MV fibroblasts vs. IRI + MV EPC; $P>0.05$ IRI + MV fibroblasts vs. IRI). (**c**) Hematoxylin/eosin staining of representative kidney sections from different experimental groups (magnification × 100).

Internalization of MVs within hypoxic TEnCs was followed by reduced apoptosis (Figure 11a) and enhanced angiogenesis on Matrigel-coated surfaces (Figure 11b). The anti-apoptotic and pro-angiogenic effects of MVs on hypoxic TEnCs was almost completely abrogated by RNase pre-treatment or by using MVs released by EPCs engineered to knock-down Dicer or by EPCs transfected with the selective anti-miR-126 and anti-miR-296 antagomiRs (Figure 11a and b). Gene array analysis revealed that MVs restored in TEnCs the expression of pro-angiogenic and

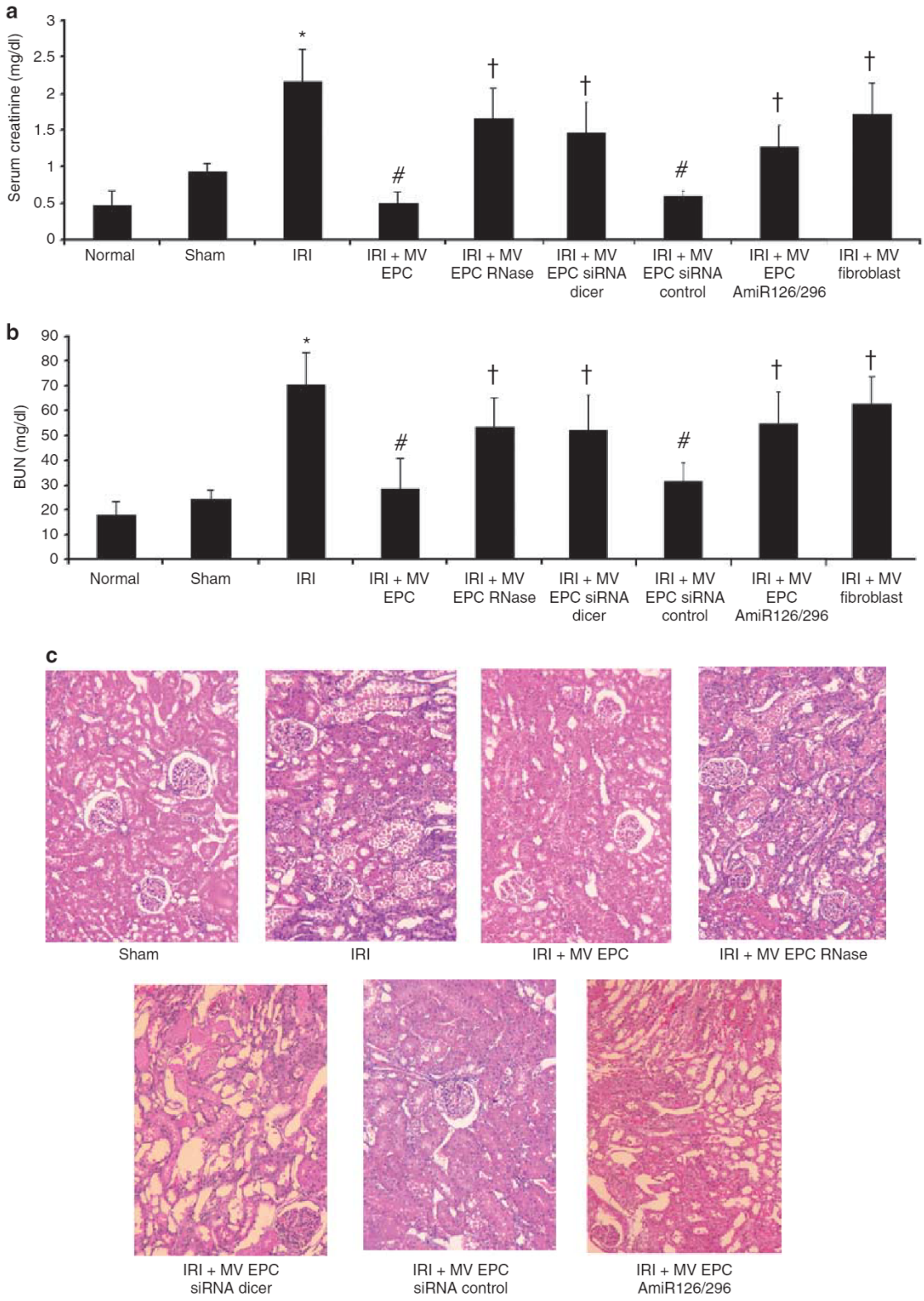

anti-apoptotic genes that were downregulated by hypoxia (Figure 11c).

Internalization of MVs within TEpC was followed by a significant inhibition of hypoxia-induced apoptosis as shown by TdT-mediated dUTP nick end labeling assay (Figure 12a) and enzyme-linked immunosorbent assay for caspase-3, -8, and -9 activities (Figure 12b). The anti-apoptotic effect of MVs was inhibited by RNase pre-treatment or by using MVs released by EPCs engineered to knock-down Dicer or by EPCs transfected with anti-miR-126 and anti-miR-296 antagomiRs. Gene array analysis revealed that MV stimulation of hypoxic TEpCs reduced the expression of inflammatory and pro-apoptotic caspases (Figure 12c) and of genes involved in both mitochondrial and death receptor pathways of apoptosis (Figure 12d).

DISCUSSION

In this study, we demonstrated that MVs derived from EPCs exert a protective effect on experimental acute renal IRI as detected by the significant decrease in serum creatinine/BUN levels and by the improvement of histological signs of microvascular and tubular injury.

EPCs were shown to induce angiogenesis and tissue repair in experimental models of acute glomerular and tubular injury.[12,13,23–25] The origin of EPCs is still a matter of debate. Some studies suggested that contamination with monocytes and platelet-derived products of EPCs derived from circulation may account for their pro-angiogenic potential.[26,27] To avoid such contamination, we purified MVs from EPCs after 3–5 passages in culture. The cells used and the derived MVs expressed the CD34 stem cell marker and markers of endothelium, but not of monocytes and platelets. Previous studies suggested that EPCs do not act via a direct trans-differentiation into mature endothelial cells, but rather by paracrine mechanisms.[10,28] We demonstrated that MVs act as a paracrine mediator as they may enter the target cells through specific receptor–ligand interactions and deliver selected patterns of mRNAs and miRNAs.[20,29–31] Moreover, MVs released from mesenchymal stem cells were shown to favor recovery from toxic and ischemic AKI.[32,33]

Table 1 | Morphologic evaluation

	Casts (n/HPF)	Tubular necrosis (n/HPF)
Normal	0	0
Sham	0	0
IRI	2.6 ± 1.2	2.9 ± 0.42
IRI+MV EPC	0.48 ± 0.21*	0.38 ± 0.16*
IRI+MV EPC RNase	2.93 ± 0.84	2.82 ± 0.89
IRI+MV EPC siRNA Dicer	2.26 ± 1.28	1.83 ± 1.19
IRI+MV EPC siRNA control	0.38 ± 0.23*	0.42 ± 0.11*
IRI+MV EPC AmiR126/296	1.36 ± 0.56*,#	1.76 ± 0.79*,#
IRI+MV fibroblasts	2.2 ± 0.94	2.3 ± 0.82

Abbreviations: EPC, endothelial progenitor; IRI, ischemia-reperfusion injury; MV, microvesicle; n/HPF, number/high-power field; siRNA, small interfering RNA.
*$P < 0.05$ IRI+EPC MV, IRI+EPC MV siRNA control or IRI+EPC MV AmiR126/296 vs. IRI; #$P < 0.05$ IRI+EPC MV AmiR126/296 vs. IRI+EPC MV.
Renal morphology score in different experimental groups: n/HPF.

Herein, we demonstrated that EPC-derived MVs protected kidney from IRI-induced functional impairment and morphologic injury. Indeed, the administration of MVs significantly decreased serum creatinine and BUN levels, renal cell apoptosis, and leukocyte infiltration. Moreover, MVs enhanced tubular cell proliferation and angiogenesis. These renoprotective effects were specific for EPC-derived MVs, as MVs obtained from human fibroblasts were ineffective.

Little is known at present about the biogenesis and the molecular composition of MVs produced by EPCs in different physiopathological states. It is supposed that the production of MVs is enhanced after appropriate stimulation. In this study, we evaluated the effects of MVs released from EPCs in basal culture conditions. However, our preliminary results indicate that hypoxia enhances the production from EPCs of MVs carrying miR-126 and miR-296 (not shown).

In vivo, MVs were detected both in endothelial cells and in tubular epithelial cells. The *in vitro* studies on isolated hypoxic TEnCs and TEpCs demonstrated that L-selectin was instrumental in MV internalization, probably through the binding to fucosylated residues or other oligosaccharide ligands known to be upregulated after IRI.[34,35]

It is known that IRI induces both microvascular and tubular injury and that TEnC dysfunction is associated with an extension phase of AKI.[36,37] Moreover, the rarefaction of renal microvascular density in the presence of sustained hypoxia is associated with an accelerated progression toward CKD.[38] On this basis, we observed the effects of EPC-derived MVs on kidneys 6 months after IRI, suggesting that MVs significantly reduced glomerulosclerosis, tubulo-interstitial fibrosis, and microvascular rarefaction, thus preserving renal function.

The results of this study suggest that the protective effects of EPC-derived MVs in experimental renal IRI seem to be associated with the triggering of angiogenesis in TEnCs and by the inhibition of apoptosis in TEpCs. Indeed, the detrimental effects induced by hypoxia on TEnCs were limited by MVs. It is interesting to note that gene array analysis of MV-stimulated hypoxic TEnCs revealed the upregulation of molecules involved in cell proliferation, angiogenesis, and inhibition of apoptosis. After an ischemic damage, TEpCs are subjected to loss of polarity with mislocalization of proteins located at the apical or at the basolateral membrane and finally to necrosis and/or apoptosis.[39,40] Herein, we showed that MVs protected TEpCs from hypoxia-induced apoptosis through the downregulation of inflammatory and pro-apoptotic caspases and by modulation of molecules involved in the mitochondrial and death receptor pathways.[41,42]

We observed that RNase treatment induced the loss of the protective effect of MVs on functional and morphological alterations induced by IRI *in vivo* and on hypoxia-induced TEnC and TEpC injury *in vitro*. The significant reduction of MV biological activities after treatment with RNase suggests a putative horizontal transfer of RNAs

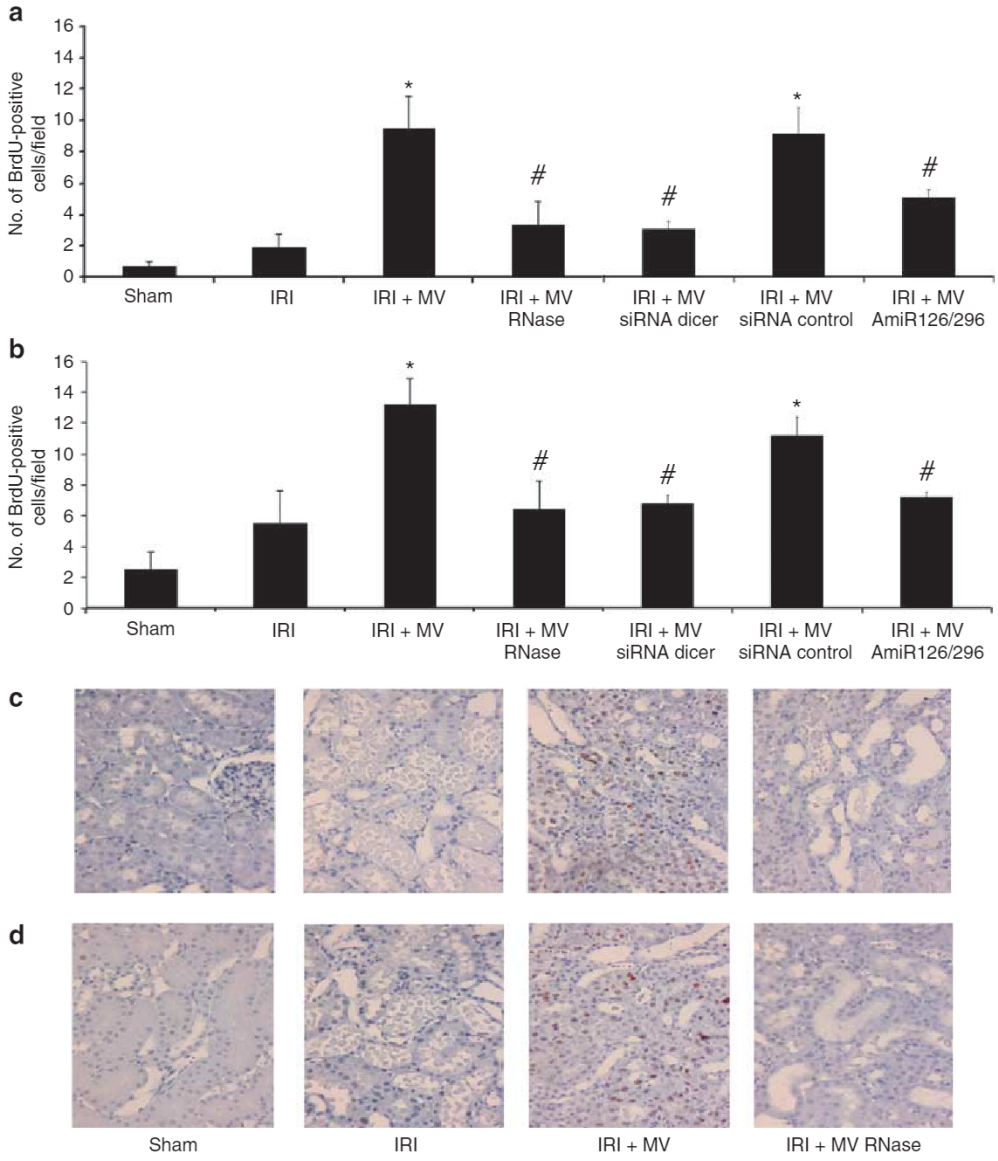

Figure 6 | Enhancement of cell proliferation induced by endothelial progenitor (EPC)-derived microvesicles (MVs) in ischemic kidneys. Count (**a**, **b**) and representative micrographs (**c**, **d**) of BrdU-positive (**a**, **c**) or PCNA-positive (**b**, **d**) cells in different experimental conditions. MVs induced a significant increase in BrdU- and PCNA-positive cells (*$P<0.05$ ischemia–reperfusion injury (IRI) + MV vs. IRI). The pre-treatment of MVs with 1 U/ml RNase or the use of MVs released from EPCs transfected with small interfering RNA (siRNA) Dicer or with antagomiRs-126/296 (AmiR126/296) significantly reduced the number of proliferating cells (#$P<0.05$ IRI + MV RNase, IRI + MV siRNA DICER or IRI + MV AmiR126/296 vs. IRI + MV). MVs released from EPCs transfected with an irrelevant control siRNA (siRNA control) significantly enhanced the number of BrdU and PCNA-positive cells (#$P<0.05$ IRI + MV siRNA control vs. IRI). All sections were counterstained with hematoxylin; original magnification × 100. BrdU, bromo deoxy uridine; PCNA, proliferating cell nuclear antigen.

from MVs to injured renal cells. It is known that MVs protect RNAs from physiological concentrations of RNase. However, as seen in previous studies,[18,20,32,33] the treatment of MVs with high concentrations of RNase inactivates the RNAs.

We previously demonstrated that MVs released from EPCs shuttle mRNAs involved in angiogenic pathways such as eNOS and Akt.[18] We now identified in EPC-derived MVs several miRNAs typical of hematopoietic stem cells and of the endothelium, which are associated with cell proliferation, angiogenesis, and inhibition of apoptosis.[43,44] In particular, MVs carried the angiomiRs miR-126 and miR-296.[45] The role of miRNAs shuttled by MVs in renal cell regeneration *in vivo* and *in vitro* was confirmed by experiments with MVs derived from EPCs previously subjected to the knock-down of Dicer, the intracellular enzyme essential for miRNA production.[46,47] These results suggest that miRNAs shuttled by MVs contribute to

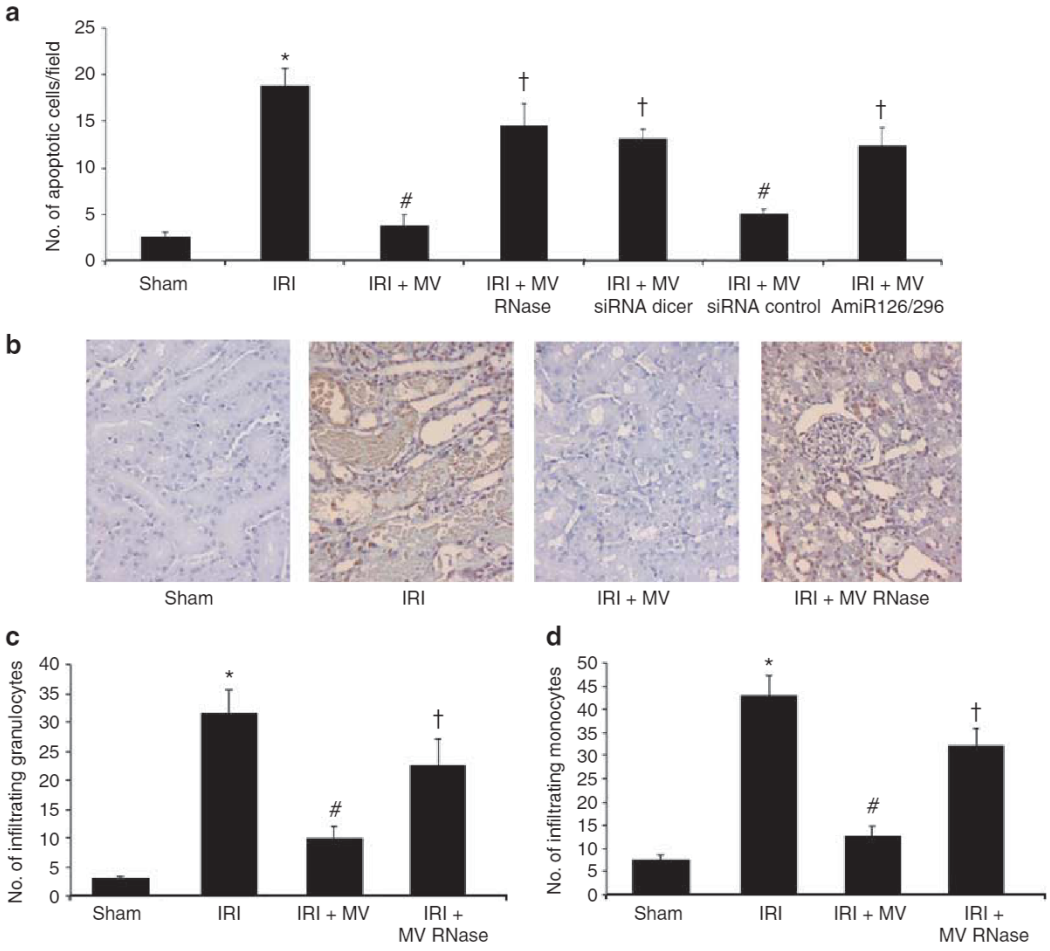

Figure 7 | Decrease in tubular cell apoptosis and leukocyte infiltration induced by endothelial progenitor (EPC)-derived microvesicles (MVs) in ischemic kidneys. (**a**, **b**) Count (**a**) and representative micrographs (**b**) of TdT-mediated dUTP nick end labeling (TUNEL)-positive cells in different experimental conditions. A significant increase in TUNEL-positive cells was observed in ischemia–reperfusion injury (IRI) in comparison with sham-treated animals (*$P<0.05$ IRI vs. sham). MVs induced a significant decrease in apoptotic cells (#$P<0.05$ IRI + MV vs. IRI). The pre-treatment of MVs with 1 U/ml RNase or the use of MVs released from EPCs transfected with small interfering RNA (siRNA) Dicer or with antagomiRs-126/296 (AmiR126/296) significantly reduced their anti-apoptotic effect (†$P<0.05$ IRI + MV RNase, IRI + MV siRNA DICER or IRI + MV AmiR126/296 vs. IRI + MV). MVs released from EPCs transfected with an irrelevant control siRNA (siRNA control) significantly reduced the number of TUNEL-positive cells (#$P<0.05$ IRI + MV siRNA control vs. IRI). All sections were counterstained with hematoxylin; original magnification: × 100. (**c**, **d**) Counts of infiltrating granulocytes (**c**) and monocytes (**d**) in different experimental conditions. IRI induced an enhancement of granulocyte and monocyte infiltration in the kidney (*$P<0.05$ IRI vs. sham), which was not observed in MV-treated animals (#$P<0.05$ IRI + MV vs. IRI). By contrast, RNase pre-treatment inhibited the decrease in granulocyte and monocyte infiltration induced by MVs (†$P<0.05$ IRI + MV RNase vs. IRI MV).

their regenerative potential. Moreover, miR-126 and miR-296 were identified to have a key role in MV-associated renoprotective effects, as MVs derived from EPCs transfected with specific antagomiRs anti-miR-126 and anti-miR-296 were less effective.

In conclusion, MVs released from EPCs exert a RNA-mediated protective effect in experimental acute renal IRI overcoming the cross-species barrier. The protective effect of MVs released from EPCs in hypoxic tissues may find therapeutic application in AKI, CKD, vascular diseases, and IRI after solid organ transplantation without the potential risks of stem cell therapy such as maldifferentiation and tumorigenesis.

MATERIALS AND METHODS

Isolation and characterization of EPCs and MVs derived from EPCs and fibroblasts

EPCs were isolated from peripheral blood mononuclear cells of healthy donors by density centrifugation and characterized as previously described.[9,18] EPCs from 3–5 passages were used in order to avoid monocyte and platelet contamination. EPCs expressed the CD34 stem cell marker and markers of endothelial cells such as CD31, KDR, CD105, and von Willebrand factor, which was detected by FACS and western blot analysis. Moreover, EPCs were able to uptake acetylated low-density lipoprotein.[9] In selected experiments, EPCs were engineered to knock-down Dicer by specific small interfering RNA (siRNA) (Santa Cruz Biotechnology, Santa Cruz, CA) or transfected with anti-miR-126 and miR-296 antagomiRs

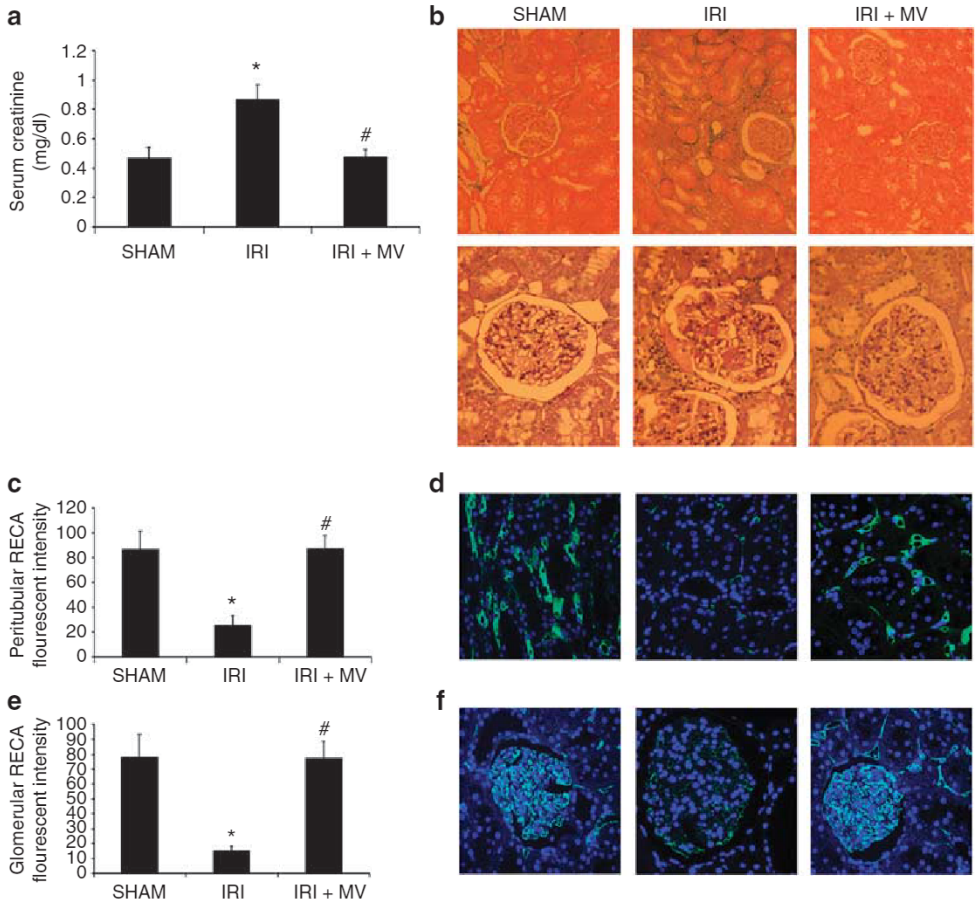

Figure 8 | Long-term preservation of renal function and inhibition of glomerulosclerosis, tubulo-interstitial fibrosis, and capillary rarefaction induced by endothelial progenitor (EPC)-derived microvesicles (MVs). (**a**) Evaluation of serum creatinine 180 days after ischemia–reperfusion injury (IRI) in different experimental groups. Rats treated with EPC-derived MVs showed lower serum creatinine levels than those observed in IRI animals (*$P<0.05$ IRI vs. sham; $^{\#}P<0.05$ IRI + MV vs. IRI). (**b**) Representative Masson's trichrome (upper panels) and hematoxylin/eosin (lower panels) staining of kidney sections of rats killed at 180 days after IRI in different experimental groups. Original magnification: × 100 in the upper panel, × 200 in the lower panel. (**c**–**f**) Mean fluorescence intensity (**c**, **e**) and representative confocal microscopy micrographs showing the staining for rat endothelial cell antigen-1 (RECA-1) antigen (**d**, **f**) in tubulo-interstitial structures (**c**, **d**) and within the glomeruli (**e**, **f**) in kidney sections of rats killed at 180 days after IRI in different experimental groups. Original magnification: × 200 in **d** and **f**: nuclei were counterstained with 2.5 μg/ml Hoechst (*$P<0.05$ IRI vs. sham; $^{\#}P<0.05$ IRI + MV vs. IRI).

(Ambion, Austin, TX). Western blot analysis for Dicer expression was performed by using an anti-Dicer polyclonal antibody (Abcam, Cambridge, UK). MVs from EPCs and control human fibroblasts were obtained from supernatants by ultracentrifugation as previously described.[18,32] MV shape and size were evaluated by transmission electron microscopy and by Nanosight technology (Nanosight, London, UK). Antigen expression on MVs was studied by FACS using antibodies directed to CD14, CD34, CD42b, L-selectin, P-selectin, CD154 (Dako, Copenhagen, Denmark), α4 integrin (Becton Dickinson, San Jose, CA), αvβ3 integrin, α6 integrin (BioLegend, San Diego, CA), and human leukocyte antigen class I and II (Santa Cruz Biotechnology). RNA extraction from MVs was performed using the mirVana isolation kit (Ambion). RNA was analyzed using the Agilent 2100 bioanalyzer (Agilent Tech, Santa Clara, CA). miRNA expression levels were analyzed using the Applied Biosystems TaqMan MicroRNA Assay Human Panel Early Access kit (Applied Biosystems, Foster City, CA) to profile 365 miRNAs by qRT-PCR (E-MEXP-2956, European Bioinformatics Institute: www.ebi.ac.uk/arrayexpress/). All reactions were performed using an Applied Biosystems 7900HT real-time PCR instrument equipped with a 384-well reaction plate (detailed protocol reported in Supplementary Information). miRNA expression levels were analyzed by qRT-PCR in a StepOne Real Time System (Ambion): 200 ng of RNA was reverse-transcribed and the complementary DNA was used to detect and quantify specific miRNAs within EPCs, fibroblasts, and MVs derived from both cell types by qRT-PCR using the miScript SYBR Green PCR Kit (Qiagen, Valencia, CA). In selected experiments, MVs were labeled with the red fluorescent dye PKH26 (Sigma-Aldrich, St Louis, MO) or treated with 1 U/ml RNase (Ambion) and then blocked with 10 U/ml RNase inhibitor (Ambion).[18]

TEnC and TEpC cultures

Primary TEpCs were isolated and characterized as previously described.[48,49] Primary TEnCs were obtained by using filters with different meshes to discard the glomeruli. Isolated cells were cultured on gelatine-coated flasks with endothelial growth factors (Lonza, Basel, Switzerland)[18]: after three passages in culture, cells

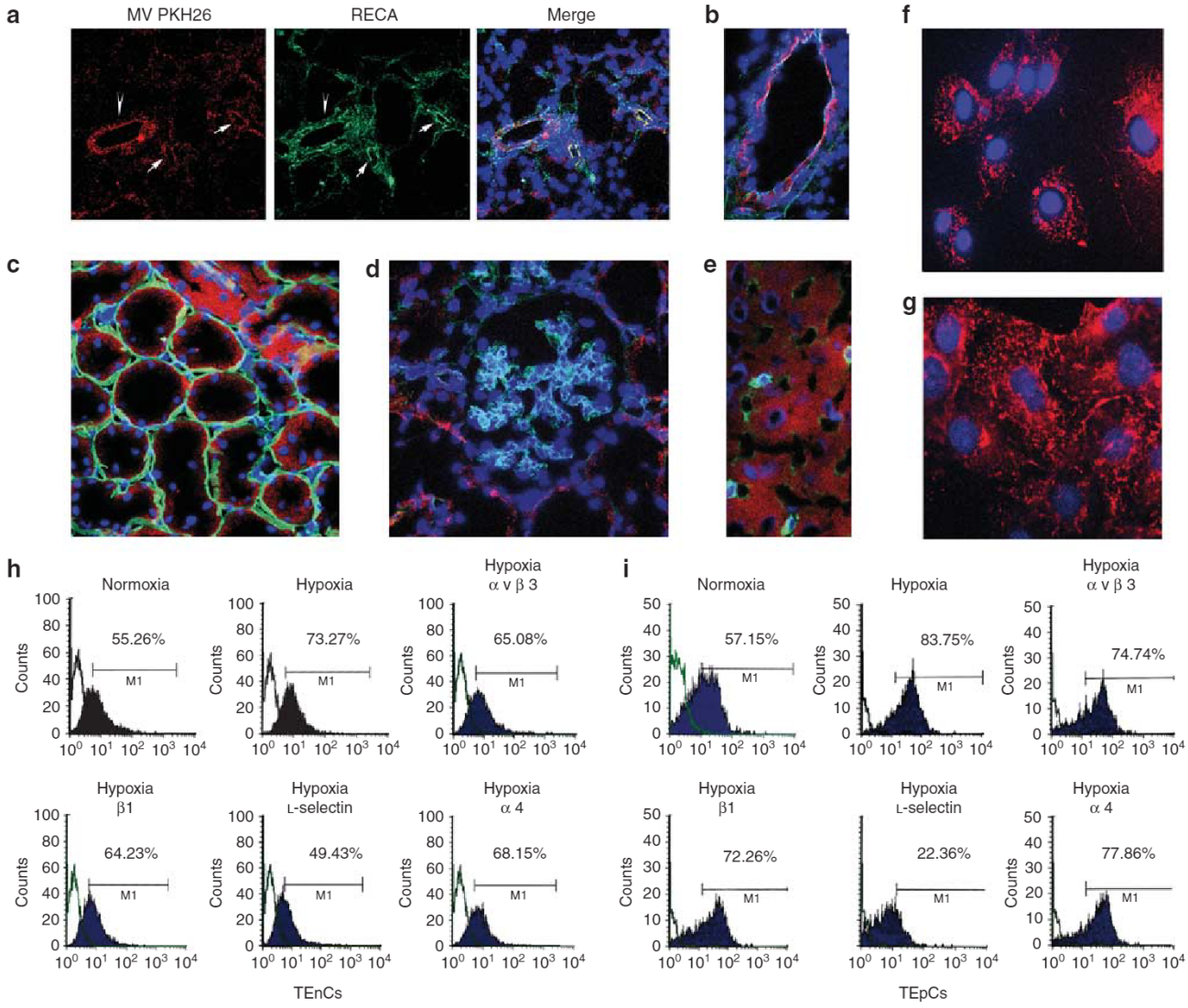

Figure 9 | *In vivo* localization and *in vitro* internalization of endothelial progenitor (EPC)-derived microvesicles (MVs) in isolated human tubular endothelial cells (TEnCs) and tubular epithelial cells (TEpCs). (**a**, **b**) Confocal microscopy analysis of PKH26-labeled MV localization in endothelial cells (green staining for rat endothelial cell antigen-1 (RECA-1); arrows) of large vessels and peritubular capillaries 2 h after injection. (**c**) Confocal microscopy analysis of PKH26-labeled MV localization in tubular epithelial cells (green staining for laminin). (**d**, **e**) Representative micrograph of PKH26-labeled MVs in kidney glomeruli (**d**) and liver (**e**) of sham-operated animals. In merge images, nuclei were counterstained with 2.5 μg/ml Hoechst. Original magnification: × 100 in **a**, **b**, **c**, and **d** and × 200 in **e**. (**f**, **g**) Confocal microscopy analysis of PKH26-labeled MVs in TEnCs (**f**) and TEpCs (**g**). Nuclei were counterstained with 2.5 μg/ml Hoechst. Original magnification × 400. (**h**, **i**) Representative FACS analysis of PKH26-labeled MV internalization in TEnCs (**h**) and TEpCs (**i**) cultured in normoxia or hypoxia in the presence or absence of different blocking monoclonal antibodies. Hypoxia enhanced MV internalization in TEnCs and TEpCs ($P<0.05$ normoxia vs. hypoxia). Anti-L-selectin mAb significantly decreased MV internalization in both cell types ($P<0.05$ hypoxia + L-selectin mAb vs. hypoxia). Three different experiments were conducted with similar results. Kolmogorov–Smirnov statistical analysis was performed on FACS data.

were further separated by magnetic cell sorting using an anti-CD31 antibody coupled to magnetic beads (MACS system, Miltenyi Biotec, Auburn, CA) and characterized for endothelial markers (CD31, CD105, and vonWillebrand factor).

Cell culture in hypoxic environment

TEnCs and TEpCs were cultured for 24 h into an airtight humidified chamber flushed with a gas mixture containing 5% CO_2, 94% N_2, and 2% O_2 at 20 atm, 37 °C.

Kidney IRI model

The experimental protocol is given in detail in Figure 4. Male Wistar rats (250 g body weight) were anesthetized by using an induction chamber with isoflurane and by intraperitoneal administration of ketamine (100 mg/kg). A subcutaneous injection of 1–2 ml normal saline was administered to replace fluid loss during the surgical procedure. After midline abdominal incision, the right kidney was removed by a sub-capsular technique. Left renal artery and vein were then occluded by using a non-traumatic vascular clamp that was

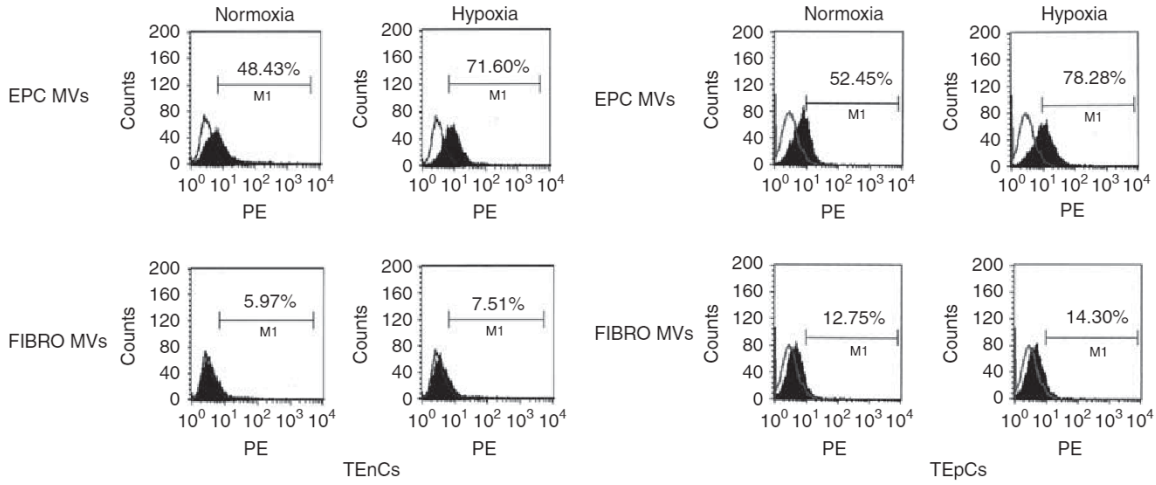

Figure 10 | Comparison of *in vitro* internalization of endothelial progenitor (EPC)- and fibroblast-derived microvesicles (MVs) in tubular endothelial cells (TEnCs) and tubular epithelial cells (TEpCs) cultured in normoxia or hypoxia. Representative fluorescence-activated cell sorting (FACS) analysis of PKH26-labeled MVs derived from EPCs or fibroblasts (FIBRO) internalized in TEnCs and TEpCs cultured in normoxia or hypoxia. Three different experiments were conducted with similar results. Kolmogorov–Smirnov statistical analysis was performed.

applied across the hilum of the kidney for 45 min. Animals were divided in the following groups: (1) normal (untreated); (2) sham-operated (right nephrectomy); (3) IRI (right nephrectomy + left renal pedicle clamp); (4) IRI + EPC MVs (right nephrectomy + left renal pedicle clamp + intravenous (i.v.) injection of 30 μg EPC MVs); (5) IRI + RNase EPC MVs (right nephrectomy + left renal pedicle clamp + i.v. injection of 30 μg EPC MVs pre-treated with 1 U/ml RNase); (6) IRI + siRNA Dicer EPC MVs (right nephrectomy + left renal pedicle clamp + i.v. injection of 30 μg MVs derived from EPCs engineered to knock-down Dicer by siRNA); (7) IRI + siRNA Control EPC MVs (right nephrectomy + left renal pedicle clamp + i.v. injection of 30 μg MVs engineered with an irrelevant siRNA); (8) IRI + AntagomiR-126/296 EPC MVs (right nephrectomy + left renal pedicle clamp + i.v. injection of 30 μg MVs derived from EPCs transfected with anti-miR-126 and anti-miR-296 antagomiRs); and (9) IRI + fibroblast MVs (right nephrectomy + left renal pedicle clamp + i.v. injection of 30 μg MVs derived from cultured fibroblasts). For all groups, MVs were diluted in 0.9% saline and injected in the tail vein immediately after IRI. Six animals from each group were killed at day 2, day 7, and day 180 (only groups 1 to 4). Kidneys were removed for histology and immunohistochemistry. For renal histology, 5-μm-thick paraffin kidney sections were routinely stained with hematoxylin/eosin or Masson's trichrome (Merck, Darmstadt, Germany). Luminal hyaline casts and cell loss (denudation of tubular basement membrane) were assessed in non-overlapping fields (up to 28 for each section) using a × 40 objective (high-power field) to evaluate the score of AKI. The number of casts and tubular profiles showing necrosis were recorded in a single-blind manner.[33] Proliferation was evaluated in rats injected with bromo deoxy uridine by using anti-bromo deoxy uridine (Dako) or anti-proliferating cell nuclear antigen (Santa Cruz Biotechnology) monoclonal antibodies.[33] TdT-mediated dUTP nick end labeling assay (Chemicon International, Temecula, CA) for the detection of apoptotic cells was performed according to manufacturer's instructions. Leukocyte infiltration was evaluated by staining with anti-monocyte (Chemicon International) or anti-granulocyte (Serotec, Oxford, UK) antibody. Immunoperoxidase staining was performed by using an anti-mouse HRP (Pierce, Rockford, IL). Confocal microscopy analysis was performed on frozen sections for localization of PKH26-labeled MVs within kidneys after staining with an anti-laminin (Sigma-Aldrich) or anti-rat endothelial cell antigen-1 antibody (Serotec).

Blood samples for measurement of serum creatinine and BUN were collected before and 2, 7, or 180 days after IRI. Creatinine concentrations were determined using a Beckman Creatinine Analyzer II (Beckman Instruments, Fullerton, CA). BUN was assessed in heparinized blood using a Beckman Synchrotron CX9 automated chemistry analyzer (Beckman Instruments).

In vitro internalization of MVs into renal cells

TEnCs and TEpCs were seeded on six-well plates in normoxic or hypoxic culture conditions and incubated with PKH26-labeled MVs derived from EPCs or fibroblasts. MV internalization was evaluated by confocal microscopy (Zeiss LSM 5 PASCAL, Jena, Germany) and FACS in the presence or absence of 1 μg/ml blocking antibodies directed to αvβ3-integrin (BioLegend), α4-integrin, α5-integrin (Chemicon International), CD29, or L-selectin (Becton Dickinson).

In vitro assays on TEnCs and TEpCs

Angiogenesis: Formation of capillary-like structures was studied on TEnCs (5×10^4) seeded for 6 h on Matrigel and observed under an inverted microscope.[50–52] *Apoptosis*: TEnCs or TEpCs were subjected to TdT-mediated dUTP nick end labeling assay (Chemicon International). Samples were analyzed under a fluorescence microscope, and green-stained apoptotic cells were counted in 10 non-consecutive microscopic fields.[50] The activities of caspase-3, -8, and -9 were assessed by enzyme-linked immunosorbent assay (Chemicon International) based on the spectrophotometric detection of the cromophore p-nitroanilide after cleavage from the labeled substrate Asp-Glu-Val-Asp-p-nitroanilide, which is recognized by caspases. Cell lysates were diluted with an appropriate reaction buffer, and Asp-Glu-Val-Asp-p-nitroanilide was added at a final concentration of 50 mol/l. Samples were analyzed in an automatized enzyme-linked immunosorbent assay reader at a wavelength of 405 nm. Each experiment was performed in triplicate.[49–50]

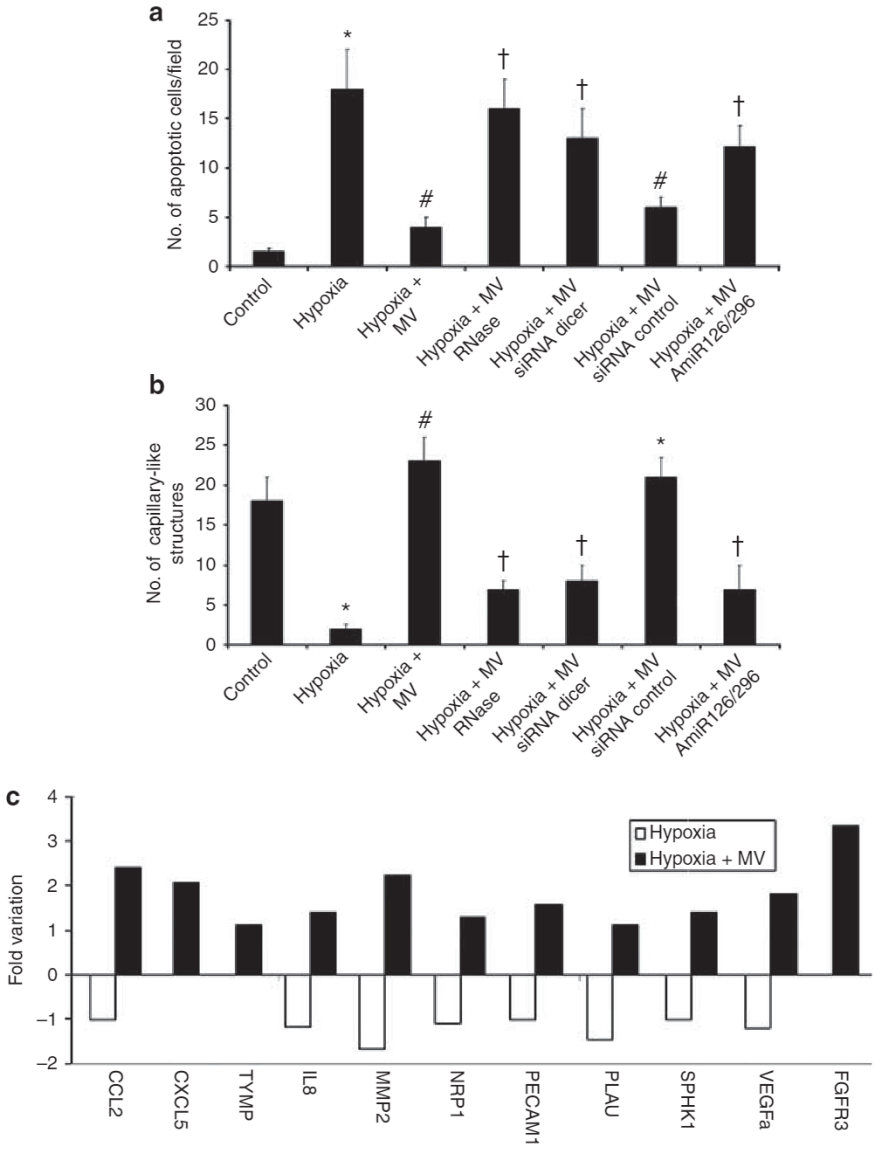

Figure 11 | Effect of endothelial progenitor (EPC)-derived microvesicles (MVs) on apoptosis, angiogenesis, and mRNA expression profile of tubular endothelial cells (TEnCs) cultured in hypoxic conditions. (**a**) TdT-mediated dUTP nick end labeling (TUNEL) assay of TEnCs cultured in different experimental conditions. With respect to normal culture (Control), hypoxia induced a significant increase in TEnC apoptosis (*$P<0.05$ hypoxia vs. control). MVs significantly decreased hypoxia-induced TEnC apoptosis ($^{\#}P<0.05$ hypoxia + MV vs. hypoxia). By contrast, preincubation of MVs with 1 U/ml RNase or the use of MVs released from EPCs transfected with small interfering RNA (siRNA) Dicer or with antagomiRs-126/296 (AmiR126/296) significantly inhibited the anti-apoptotic effect of MVs ($^{\dagger}P<0.05$ hypoxia + MV RNase, hypoxia + MV siRNA Dicer or hypoxia + MV AmiR126/296 vs. hypoxia + MV). MVs released from EPCs transfected with an irrelevant control siRNA (siRNA control) significantly reduced the number of apoptotic cells ($^{\#}P<0.05$ hypoxia + MV siRNA control vs. hypoxia). Results are given as mean ± s.d. of green-stained apoptotic cells in 10 microscopic fields (magnification × 100) of five independent experiments. (**b**) *In vitro* angiogenesis assay of TEnCs cultured on Matrigel-coated plates in different experimental conditions. With respect to normal culture (control), hypoxia induced a significant decrease in TEnC angiogenesis (*$P<0.05$ hypoxia vs. control). MVs enhanced angiogenesis of hypoxic TEnCs ($^{\#}P<0.05$ hypoxia + MV vs. hypoxia). By contrast, preincubation of MVs with 1 U/ml RNase or the use of MVs released from EPCs transfected with siRNA Dicer or with antagomiRs-126/296 (AmiR126/296) significantly inhibited the pro-angiogenic effect of MVs ($^{\dagger}P<0.05$ hypoxia + MV RNase, hypoxia + MV siRNA Dicer or hypoxia + MV AmiR126/296 vs. hypoxia + MV). MVs released from EPCs transfected with an irrelevant control siRNA (siRNA control) significantly increased TenC angiogenesis ($^{\#}P<0.05$ hypoxia + MV siRNA control vs. hypoxia). Results are given as mean ± s.d. of 20 different microscopic fields (magnification × 100). Three independent experiments were conducted with similar results. (**c**) Gene array profiling of TEnCs cultured in different experimental conditions (angiogenesis-related genes). The graph shows the fold variation of angiogenesis-related genes between TEnCs cultured in hypoxia in the absence (white columns) or presence (black columns) of MVs in comparison with TEnCs cultured in normoxic conditions. Samples were normalized for the signals found in housekeeping genes (actin, GAPDH). Three independent experiments were conducted with similar results. Gene table: CCL2, chemokine (C-C motif) ligand 2; CXCL5, C-X-C motif chemokine 5; FGFR3, fibroblast growth factor receptor 3; IL8, interleukin-8; MMP2, matrix metalloproteinase-2; NRP1, neuropilin-1; PECAM1, platelet endothelial cell adhesion molecule (CD31); PLAU, urokinase-type plasminogen activator; SPHK1, sphingosine kinase 1; TYMP, thymidine phosphorylase; VEGFa, vascular endothelial growth factor A.

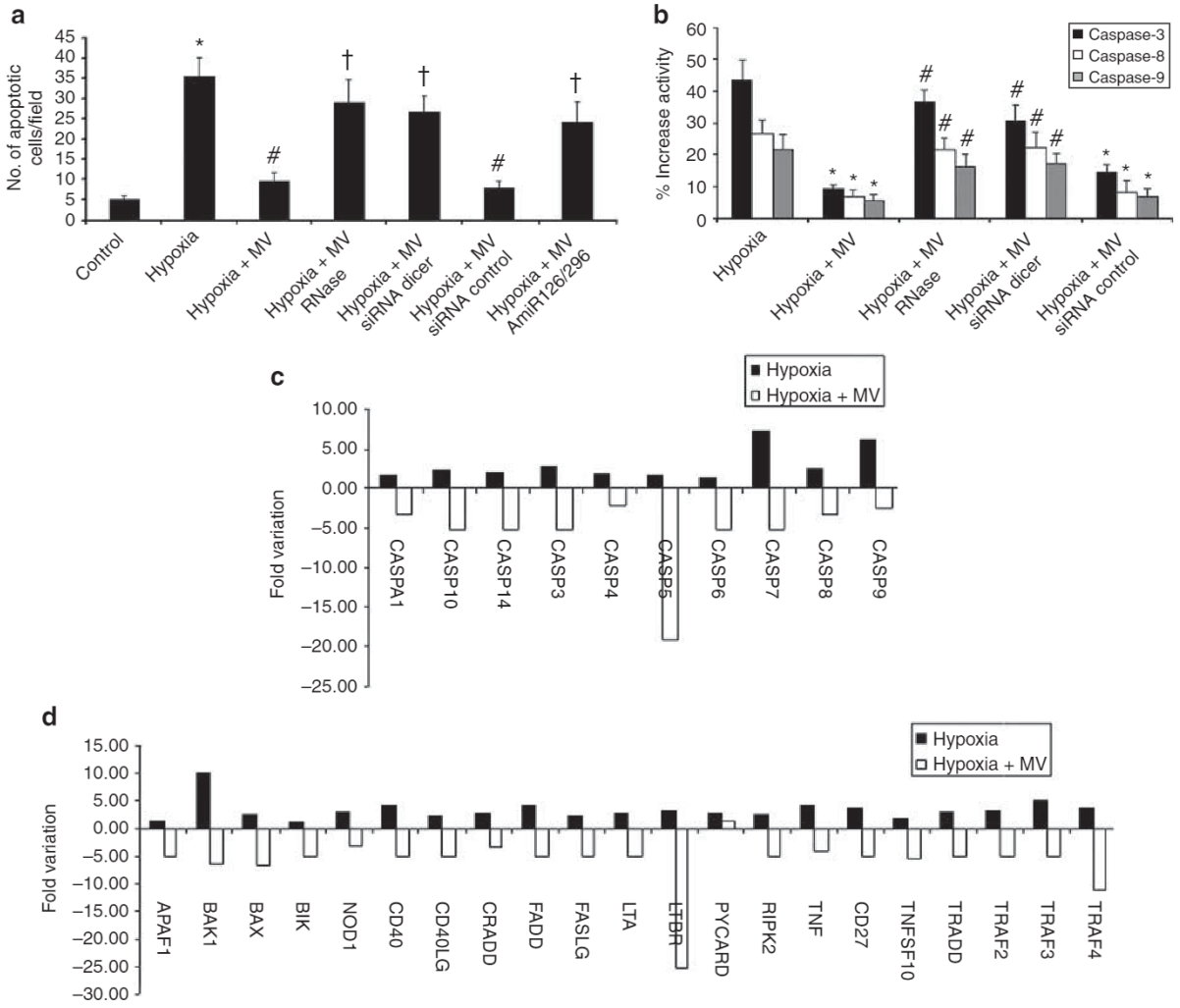

Figure 12 | Effect of endothelial progenitor (EPC)-derived microvesicles (MVs) on apoptosis and mRNA expression profile of tubular epithelial cells (TEpCs) cultured in hypoxic conditions. (**a**, **b**) TdT-mediated dUTP nick end labeling (TUNEL) assay (**a**) and enzyme-linked immunosorbent assay (ELISA) for caspase-3, -8, and -9 activities (**b**) of TEpCs cultured in different experimental conditions. Hypoxia induced a significant increase in TEpC apoptosis ($^{*}P<0.05$ hypoxia vs. control). MVs significantly decreased hypoxia-induced TEpC apoptosis ($^{\#}P<0.05$ hypoxia + MV vs. hypoxia). By contrast, preincubation of MVs with 1 U/ml RNase or the use of MVs released from EPCs transfected with small interfering RNA (siRNA) Dicer or with antagomiRs-126/296 (AmiR126/296) significantly inhibited the anti-apoptotic effect of MVs ($^{\dagger}P<0.05$ hypoxia + MV RNase, hypoxia + MV siRNA Dicer or hypoxia + MV AmiR126/296 vs. hypoxia + MV). MVs released from EPCs transfected with an irrelevant control siRNA (siRNA Control) significantly reduced the number of apoptotic cells ($^{\#}P<0.05$ hypoxia + MV siRNA control vs. hypoxia). Results are given as mean ± s.d. of green-stained apoptotic cells in 10 microscopic fields (magnification × 100) of five independent experiments. Similar results were observed for caspase activities ($^{*}P<0.05$ hypoxia + MV or hypoxia + MV siRNA control vs. hypoxia; $^{\#}P<0.05$ hypoxia + MV RNase or hypoxia + MV siRNA Dicer vs. hypoxia + MV). Results are given as mean ± s.d. of five independent experiments and expressed as percentage increase in caspase activity with respect to normal culture conditions. (**c**, **d**) Gene array profiling of TEpCs cultured in different experimental conditions (apoptosis-related genes). The graph shows the fold variation of apoptosis-related genes between TEpCs cultured in hypoxia in the absence (black columns) or presence (white columns) of MVs in comparison with TEpCs cultured in normoxic conditions. Samples were normalized for the signals found in housekeeping genes (actin, GAPDH). Three independent experiments were conducted with similar results. Gene table in **c**: CASP1, caspase-1; CASP10, caspase-10; CASP14, caspase-14; CASP3, caspase-3; CASP4, caspase-4; CASP5, caspase-5; CASP6, caspase-6; CASP7, caspase-7; CASP8, caspase-8; CASP9, caspase-9. Gene table in **d**: APAF1, apoptotic protease-activating factor 1; BAK1, BCL2-antagonist/killer 1; BAX, BCL2-associated X protein; BIK, Bcl-2-interacting killer; NOD1, nucleotide-binding oligomerization domain-containing protein 1; CD27, CD 27; CD40, CD 40; CD40LG, CD40 ligand (CD154); CRADD, death domain (CARD/DD)-containing protein; FADD, Fas-associated protein with death domain; FASLG, Fas ligand (TNF superfamily, member 6); LTA, lymphotoxin alpha; LTBR, lymphotoxin beta receptor (TNFR superfamily, member 3); PYCARD, apoptosis-associated speck-like protein containing a CARD or ASC; RIPK2, receptor-interacting serine/threonine-protein kinase 2; TNF, tumor necrosis factor; TNFSF10, TNF-related apoptosis-inducing ligand (TRAIL); TRADD, tumor necrosis factor receptor type 1-associated DEATH domain protein; TRAF2, TNF receptor-associated factor 2; TRAF3, TNF receptor-associated factor 3; TRAF4, TNF receptor-associated factor 4.

Gene array analysis

The human GEarray kit for the study of angiogenesis in TEnCs and apoptosis in TEpCs (SuperArray, Bethesda, MD) was used to characterize the gene expression profile of cells cultured in normoxia or hypoxia in the presence or absence of MVs. Microarray data archive: (E-MEXP-2972 for TEnC angiogenesis and E-MEXP-3086 for TEpC apoptosis, European Bioinformatics Institute: www.ebi.ac.uk/arrayexpress/).

Statistical analysis

All data of different experimental procedures are expressed as average ± s.d. Statistical analysis was performed by Kruskal–Wallis statistical test for *in vivo* studies and by Student's *t*-test or analysis of variance with Newmann–Keuls or Dunnet's multicomparison test where appropriate for *in vitro* experiments. For FACS data, the Kolmogorov–Smirnov nonparametric statistical test was performed.

DISCLOSURE

SG, SB, MCD, and GC received funding for research from Fresenius Medical Care. CT (Fresenius Medical Care) is employed by a commercial company and contributed to the study as researcher. VC, MCD, SB, CT, and GC are named as inventors in related patents.

ACKNOWLEDGMENTS

This work was supported by Italian Government Miur PRIN project, Regione Piemonte, Piattaforme Biotecnologiche PiSTEM project and Converging Technologies NanoIGT project, Ricerca Finalizzata and Local University Grants (ex-60%).

SUPPLEMENTARY MATERIAL

Supplementary Information 1. Supplementary methods.
Table S1. miRNA array analysis in EPCs (A: pro-angiogenic; B: proliferative; C: anti-apoptotic; D: stem cells).
Table S2. miRNA array analysis in EPC MVs (A: pro-angiogenic; B: proliferative; C: anti-apoptotic; D: stem cells).
Supplementary material is linked to the online version of the paper at http://www.nature.com/ki

REFERENCES

1. Mehta RL, Pascual MT, Soroko S *et al.* Program to improve care in acute renal disease. Spectrum of acute renal failure in the intensive care unit: the PICARD experience. *Kidney Int* 2004; **66**: 1613–1621.
2. Hoste EA, Kellum JA, Katz NM *et al.* Epidemiology of acute kidney injury. *Contrib Nephrol* 2010; **165**: 1–8.
3. Chawla LS, Amdur RL, Amodeo S *et al.* The severity of acute kidney injury predicts progression to chronic kidney disease. *Kidney Int* 2011; **79**: 1361–1369.
4. Benigni A, Morigi M, Remuzzi G *et al.* Kidney regeneration. *Lancet* 2010; **375**: 1310–1317 Review.
5. Herrera MB, Bussolati B, Bruno S *et al.* Mesenchymal stem cells contribute to the renal repair of acute tubular epithelial injury. *Int J Mol Med* 2004; **14**: 1035–1041.
6. Morigi M, Introna M, Imberti B *et al.* Human bone marrow mesenchymal stem cells accelerate recovery of acute renal injury and prolong survival in mice. *Stem Cells* 2008; **26**: 2075–2082.
7. Bussolati B, Bruno S, Grange C. Isolation of renal progenitor cells from adult human kidney. *Am J Pathol* 2005; **166**: 545–555.
8. Asahara T, Murohara T, Sullivan A *et al.* Isolation of putative progenitor endothelial cells for angiogenesis. *Science* 1997; **275**: 964–967.
9. Biancone L, Cantaluppi V, Duò D *et al.* Role of L-selectin in the vascular homing of peripheral blood-derived endothelial progenitor cells. *J Immunol* 2004; **173**: 5268–5274.
10. Zampetaki A, Kirton JP, Xu Q. Vascular repair by endothelial progenitor cells. *Cardiovasc Res* 2008; **78**: 413–421.
11. Charwat S, Gyöngyösi M, Lang I *et al.* Role of adult bone marrow stem cells in the repair of ischemic myocardium: current state of the art. *Exp Hematol* 2008; **36**: 672–680.
12. Uchimura H, Marumo T, Takase O *et al.* Intrarenal injection of bone marrow-derived angiogenic cells reduces endothelial injury and mesangial cell activation in experimental glomerulonephritis. *J Am Soc Nephrol* 2005; **16**: 997–1004.
13. Kwon O, Miller S, Li N *et al.* Bone marrow-derived endothelial progenitor cells and endothelial cells may contribute to endothelial repair in the kidney immediately after ischemia-reperfusion. *J Histochem Cytochem* 2010; **58**: 687–694.
14. Patschan D, Plotkin M, Goligorsky MS. Therapeutic use of stem and endothelial progenitor cells in acute renal injury: ça ira. *Curr Opin Pharmacol* 2006; **6**: 176–183.
15. Li B, Cohen A, Hudson TE *et al.* Mobilized human hematopoietic stem/progenitor cells promote kidney repair after ischemia/reperfusion injury. *Circulation* 2010; **121**: 2211–2220.
16. Goligorsky MS, Yasuda K, Ratliff B. Dysfunctional endothelial progenitor cells in chronic kidney disease. *J Am Soc Nephrol* 2010; **21**: 911–919.
17. Yang Z, von Ballmoos MW, Faessler D *et al.* Paracrine factors secreted by endothelial progenitor cells prevent oxidative stress-induced apoptosis of mature endothelial cells. *Atherosclerosis* 2010; **211**: 103–109.
18. Deregibus MC, Cantaluppi V, Calogero R *et al.* Endothelial progenitor cell derived microvesicles activate an angiogenic program in endothelial cells by a horizontal transfer of mRNA. *Blood* 2007; **110**: 2440–2448.
19. Ratajczak J, Wysoczynski M, Hayek F *et al.* Membrane-derived microvesicles: important and underappreciated mediators of cell-to-cell communication. *Leukemia* 2006; **20**: 1487–1495.
20. Ratajczak J, Miekus K, Kucia M *et al.* Embryonic stem cell-derived microvesicles reprogram hematopoietic progenitors: evidence for horizontal transfer of mRNA and protein delivery. *Leukemia* 2006; **20**: 847–856.
21. De Broe ME, Wieme RJ, Logghe GN *et al.* Spontaneous shedding of plasma membrane fragments by human cells *in vivo* and *in vitro*. *Clin Chim Acta* 1977; **81**: 237–245.
22. Valadi H, Ekström K, Bossios A *et al.* Exosome-mediated transfer of mRNAs and microRNAs is a novel mechanism of genetic exchange between cells. *Nat Cell Biol* 2007; **9**: 654–659.
23. Ikarashi K, Li B, Suwa M *et al.* Bone marrow cells contribute to regeneration of damaged glomerular endothelial cells. *Kidney Int* 2005; **67**: 1925–1933.
24. Daniel C, Amann K, Hohenstein B *et al.* Thrombospondin 2 functions as an endogenous regulator of angiogenesis and inflammation in experimental glomerulonephritis in mice. *J Am Soc Nephrol* 2007; **18**: 788–798.
25. Becherucci F, Mazzinghi B, Ronconi E *et al.* The role of endothelial progenitor cells in acute kidney injury. *Blood Purif* 2009; **27**: 261–270.
26. Aharon A, Tamari T, Brenner B. Monocyte-derived microparticles and exosomes induce procoagulant and apoptotic effects on endothelial cells. *Thromb Haemost* 2008; **100**: 878–885.
27. Prokopi M, Pula G, Mayr U *et al.* Proteomic analysis reveals presence of platelet microparticles in endothelial progenitor cell cultures. *Blood* 2009; **114**: 723–732.
28. Yoder MC, Mead LE, Prater D *et al.* Redefining endothelial progenitor cells via clonal analysis and hematopoietic stem/progenitor cell principals. *Blood* 2007; **109**: 1801–1809.
29. De Broe ME, Wieme RJ, Logghe GN *et al.* Spontaneous shedding of plasma membrane fragments by human cells *in vivo* and *in vitro*. *Clin Chim Acta* 1977; **81**: 237–245.
30. Schorey JS, Bhatnagar S. Exosome function: from tumor immunology to pathogen biology. *Traffic* 2008; **9**: 871–881.
31. Quesenberry PJ, Dooner MS, Aliotta JM. Stem cell plasticity revisited: the continuum marrow model and phenotypic changes mediated by microvesicles. *Exp Hematol* 2010; **38**: 581–592.
32. Bruno S, Grange C, Deregibus MC *et al.* Mesenchymal stem cell-derived microvesicles protect against acute tubular injury. *J Am Soc Nephrol* 2009; **20**: 1053–1067.
33. Gatti S, Bruno S, Deregibus MC *et al.* Microvesicles derived from human adult mesenchymal stem cells protect against ischaemia-reperfusion-induced acute and chronic kidney injury. *Nephrol Dial Transplant* 2011; **26**: 1474–1483.
34. Burne MJ, Rabb H. Pathophysiological contributions of fucosyltransferases in renal ischemia reperfusion injury. *J Immunol* 2002; **169**: 2648–2652.
35. Rabb H, O'Meara YM, Maderna P *et al.* Leukocytes, cell adhesion molecules and ischemic acute renal failure. *Kidney Int* 1997; **51**: 1463–1468.

36. Molitoris BA, Sutton TA. Endothelial injury and dysfunction: role in the extension phase of acute renal failure. *Kidney Int* 2004; **66**: 496–499.
37. Sutton TA, Fisher CJ, Molitoris BA. Microvascular endothelial injury and dysfunction during ischemic acute renal failure. *Kidney Int* 2002; **62**: 1539–1549.
38. Legrand M, Mik EG, Johannes T *et al.* Renal hypoxia and dysoxia after reperfusion of the ischemic kidney. *Mol Med* 2008; **14**: 502–516.
39. Bonventre JV, Weinberg JM. Recent advances in the pathophysiology of ischemic acute renal failure. *J Am Soc Nephrol* 2003; **14**: 2199–2210.
40. Bonventre JV. Dedifferentiation and proliferation of surviving epithelial cells in acute renal failure. *J Am Soc Nephrol* 2003; **14**: S55–S61.
41. Kaushal GP, Basnakian AG, Shah SV. Apoptotic pathways in ischemic acute renal failure. *Kidney Int* 2004; **66**: 500–506.
42. Sheridan AM, Bonventre JV. Cell biology and molecular mechanisms of injury in ischemic acute renal failure. *Curr Opin Nephrol Hypertens* 2000; **9**: 427–434 Review.
43. Nelson P, Kiriakidou M, Sharma A *et al.* The microRNA world: small is mighty. *Trends Biochem Sci* 2003; **28**: 534–540.
44. Camussi G, Deregibus MC, Bruno S *et al.* Exosomes/microvesicles as a mechanism of cell-to-cell communication. *Kidney Int* 2010; **78**: 838–848.
45. Wang S, Olson EN. AngiomiRs–key regulators of angiogenesis. *Curr Opin Genet Dev* 2009; **19**: 205–211.
46. Jaskiewicz L, Filipowicz W. Role of dicer in posttranscriptional RNA silencing. *Curr Top Microbiol Immunol* 2008; **320**: 77–97.
47. Saal S, Harvey SJ. MicroRNAs and the kidney: coming of age. *Curr Opin Nephrol Hypertens* 2009; **18**: 317–323.
48. Conaldi PG, Biancone L, Bottelli A *et al.* HIV-1 kills renal tubular epithelial cells *in vitro* by triggering an apoptotic pathway involving caspase activation and Fas upregulation. *J Clin Invest* 1998; **102**: 2041–2049.
49. Cantaluppi V, Biancone L, Romanazzi GM *et al.* Macrophage stimulating protein may promote tubular regeneration after acute injury. *J Am Soc Nephrol* 2008; **19**: 1904–1918.
50. Cantaluppi V, Biancone L, Romanazzi GM *et al.* Antiangiogenic and immunomodulatory effects of rapamycin on islet endothelium: relevance for islet transplantation. *Am J Transplant* 2006; **6**: 2601–2611.
51. Boccellino M, Biancone L, Cantaluppi V *et al.* Effect of platelet-activating factor receptor expression on CHO cell motility. *J Cell Physiol* 2000; **183**: 254–264.
52. Biancone L, Cantaluppi V, Segoloni G *et al.* Role of platelet-activating factor in functional alterations induced by xenoreactive antibodies in porcine endothelial cells. *Transplantation* 2000; **70**: 1198–1205.